scientific reports

Check for updates

OPEN

Valosin-containing protein modulator KUS121 protects retinal neurons in a rat model of anterior ischemic optic neuropathy

Chinami Kikkawa[1,2], Hanako Ohashi Ikeda[1,3]✉, Masayuki Hata[1], Sachiko Iwai[1] & Akitaka Tsujikawa[1]

Ischemic optic neuropathy is a leading cause of sudden vision loss, particularly in elderly individuals, with no available effective treatments. Ischemia-induced irreversible damage to optic nerve fibers highlights the need for novel therapies with neuroprotective potential. Therefore, we investigated the effects of modulating valosin-containing proteins by regulating their intracellular ATPase activity in a rat model of anterior ischemic optic neuropathy. Intravitreal injection of KUS121 (Kyoto University Substance 121), a valosin-containing protein modulator, significantly reduced retinal thinning, retinal ganglion cell death, and optic nerve fiber loss. Morphological and histopathological analyses showed that KUS121 treatment prevented the disorganization, swelling, and loss of myelin. Notably, KUS121 demonstrated strong neuroprotective effects even when administered immediately after the induction of ischemic optic neuropathy. Mechanistically, the neuroprotective effect of KUS121 can be attributed to the suppression of endoplasmic reticulum stress, as evidenced by reduced expression of the C/EBP homologous protein, a marker of endoplasmic reticulum stress, following ischemic injury. Conclusively, KUS121 is promising as a therapeutic option for ischemic optic neuropathy and other ischemia-related neurodegenerative conditions.

Keywords Anterior ischemic optic neuropathy, Endoplasmic reticulum stress, Neuroprotection, Intravitreal injection, Valosin-containing protein modulation

Ischemic optic neuropathy (ION) is a major cause of vision impairment and is classified into anterior ischemic optic neuropathy (AION) and posterior ischemic optic neuropathy (PION)[1]. AION, primarily caused by ischemia of the posterior ciliary artery, is further divided into arteritis-associated AION (A-AION) and non-arteritis-associated AION (NA-AION) subtypes[1,2].

NA-AION, the most common type of ION, results from ischemic damage to the optic nerve head[1], often linked to small-vessel disease or vascular insufficiency. This condition compromises blood flow to the optic nerve head, leading to ischemia and subsequent infarction. Although the exact mechanisms of NA-AION development are not fully understood, vascular compromise, endothelial dysfunction, and microvascular abnormalities are considered to be involved in its pathogenesis. Systemic conditions such as hypertension, diabetes, and atherosclerosis may increase susceptibility to NA-AION by exacerbating vascular perfusion deficits in the optic nerve head. Ultimately, ischemic damage to the optic nerve head results in optic nerve dysfunction, typically presenting as acute to subacute painless vision loss, often accompanied by optic disc edema and altitudinal visual field defects. Currently, there are no established treatments for NA-AION[3].

In contrast, A-AION is caused by vasculitis, most commonly giant cell arteritis, which leads to inflammation and occlusion of the posterior ciliary artery. Without prompt treatment, A-AION can cause severe, irreversible vision loss. Early diagnosis and immediate systemic corticosteroid therapy are critical to prevent blindness[2].

Ischemia is also a major cause or exacerbating factor in several ocular diseases, including diabetic retinopathy, retinal artery occlusion, optic neuropathy, and glaucoma. Currently, no treatment, including that for NA-AION, can effectively protect neurons from ischemic damage[2,3]. Endoplasmic reticulum (ER) stress has been proposed as a key mechanism in ischemic neuronal cell death[4,5]. Neurons have highly developed endoplasmic reticula,

[1]Department of Ophthalmology and Visual Sciences, Kyoto University Graduate School of Medicine, Sakyo-ku, Kyoto 606-8507, Japan. [2]Product Development Division, Santen Pharmaceutical Co., Ltd, Nara, Japan. [3]Department of Ophthalmology, Osaka Medical and Pharmaceutical University, Osaka, Japan. ✉email: hanakoi@kuhp.kyoto-u.ac.jp

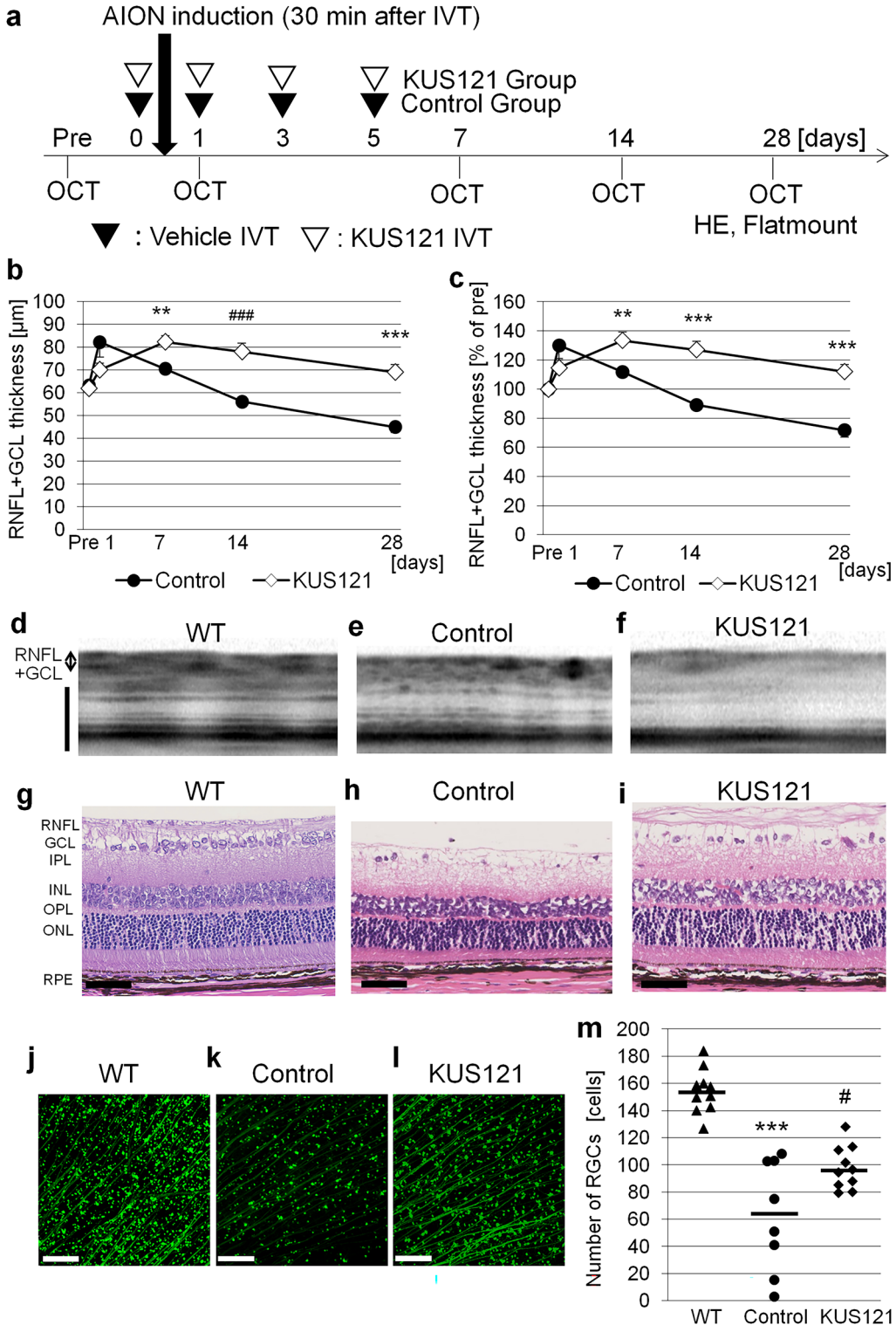

and ischemia triggers ER stress, leading to neuronal death[6,7]. C/EBP homologous protein (CHOP), an ER stress-inducing molecule, has been identified as a major mediator of apoptosis in neuroischemia[5]. Thus, novel agents that reduce ER stress may exert neuroprotection in ischemic diseases.

In a previous study, we showed that Kyoto University Substances (KUSs), novel compounds developed as ATPase inhibitors of valosin-containing proteins (VCP), act as ''VCP modulators" or ''ATP regulators" by selectively inhibiting the ATPase activity of VCP without affecting their cellular functions[8]. These VCP modulators exhibit strong neuroprotective effects on retinal photoreceptors and ganglion cells in vivo by reducing ER stress[8–11]. In a clinical trial, following intravitreal administration, KUS121 (one of the most potent neuroprotectants among the KUSs) has been found to safely and effectively improve visual function in central retinal artery occlusion[12]. Considering that ER stress-induced cell death is a major factor in AION pathogenesis, we investigated the therapeutic effects of KUS121 in a rat model of AION (rAION).

◀**Fig. 1**. Effects of pre-intravitreal injection of KUS121 in a rat model of anterior ischemic optic neuropathy (rAION). **a** Schematic of the experimental schedule. AION: anterior ischemic optic neuropathy, OCT: optical coherent tomography, HE: hematoxylin eosin-staining, IVT: intravitreal injection. **b**, **c** Retinal thickness, including the retinal nerve fiber layer (RNFL) and ganglion cell layer (GCL), (b) and its percent change compared to pre-treatment value (c) in AION rats intravitreally injected with KUS121 ($n = 10$, squares) or vehicle (control) ($n = 8$, circles). Error bars indicate standard error (SE). $^{**}P < 0.01$, $^{***}P < 0.001$ vs. control (Student's t-test), $^{\#\#\#}P < 0.001$ vs. control (Aspin–Welch's t-test). **d–f** Representative OCT images of wild-type rats (WT, d) and AION rats injected with vehicle (control, e) or KUS121 (f). The double arrows indicate the layers, including the RNFL and GCL. Bar = 200 µm. **g–i** Representative images of HE-stained retinal sections of WT rats (WT, g) and AION rats injected with vehicle (control, h) or KUS121 (i). IPL: inner plexiform layer, INL: inner nuclear layer, OPL: outer plexiform layer, ONL: outer nuclear layer, RPE: retinal pigment epithelium. Bar = 50 µm. **j–l** Representative images of flat-mounted retinas of WT (j) and AION rats injected with vehicle (control, k) or KUS121 (l) at 28 days post-AION induction. Bar = 100 µm. **m** Number of GFP-positive retinal ganglion cells (RGCs) in WT ($n = 10$) and AION rats injected with vehicle (control, $n = 8$) or KUS121 ($n = 10$) at 28 days post-AION induction. GFP-positive RGCs were manually counted within four 500-µm squares located 2000 µm from the optic nerve head center (supplementary Fig. S1f). Bars indicate average. *** $P < 0.001$ vs. WT, $^{\#}P = 0.021$ vs. control (Tukey's HSD test).

Results

Evaluating time-dependent changes in the rAION model

To induce AION in rats, ischemia was induced in the optic nerve head of *Thy1*-green fluorescent protein (GFP) rats[13]using laser irradiation[14–16]. Spectral-domain optical coherence tomography (OCT) was employed to monitor AION-induced retinal damage and atrophy over time, focusing on changes in total retinal thickness, inner retinal layers (the retinal nerve fiber layer [RNFL] + ganglion cell layer [GCL] + inner plexiform layer [IPL]), and RNFL + GCL (Supplementary Fig. S1a). Notably, total retinal thickness increased at 1 day post-AION induction, followed by a steady decrease (returning to baseline thickness by day 7) until 28 days post-induction (Supplementary Fig. S1b-d). In contrast, the thicknesses of RNFL + GCL and RNFL + GCL + IPL peaked at 3 and 2 days post-AION induction, respectively (Supplementary Fig. S1c, d). Fluorescein fundus photography showed that the number of GFP-positive retinal ganglion cells (RGCs) and nerve fibers decreased rapidly until 14 days post-induction, with minimal reduction observed on day 28 (Supplementary Fig. S1e). Retinal flat mounts revealed that only a few retinal nerve fibers and RGCs remained in the rAION model at 28 days post-AION induction, indicating RGC loss (Supplementary Fig. S1f). Electroretinogram (ERG) analysis showed no significant changes in the amplitude or latency of the a- and b-waves at all points, indicating no detectable alterations in visual function in the model group (Supplementary Fig. S2).

Effect of intravitreal administration of KUS121 in the rAION model

To investigate the therapeutic effect of KUS121, rats in the AION group were intravitreally administered KUS121 or vehicle (control group) 30 min before, and 1, 3, and 5 days post-AION induction (Fig. 1a). In the control group, the inner retinal thickness (RNFL + GCL + IPL) and total retinal thickness increased at 1 day post-induction and decreased gradually thereafter. In the KUS121-treated group, an increase was observed in retinal thickness at 7 days post-induction, followed by a gradual decrease to nearly pre-AION levels at 28 days post-induction (Fig. 1b–f, Supplementary Fig. S3). Notably, the retinal thickness was significantly higher in the KUS121 group than in the control group at 7–28 days post-induction (day 28: RNFL + GCL thickness, 68.9 ± 3.4 µm vs. 44.9 ± 2.4 µm, $P < 0.001$; Fig. 1b–f). Hematoxylin and eosin staining at 28 days post-induction revealed that KUS121 treatment suppressed the thinning of inner retinal layers and RGC loss (Fig. 1g–i). Additionally, KUS121 treatment significantly preserved RGCs and nerve fibers compared to the control (97.7 ± 5.0 cells vs. 62.4 ± 14.5 cells, $P = 0.021$; Fig. 1j–m).

To investigate the potential clinical relevance of KUS121, we examined the therapeutic effect of KUS121 immediately after AION induction. In this experiment (Fig. 2a), on the day following AION induction, the rats were intravitreally administered KUS121 and divided into two groups based on retinal edema at 1 day post-AION induction. Thereafter, the rats were treated with a vehicle (control) and KUS121 at 1, 3, and 5 days post-AION induction. Although the retinal thickness increased at 1 day post-induction and decreased thereafter in both groups, the decrease was milder in the KUS121 group (Fig. 2b–f, Supplementary Fig. S4). The retinal thickness was below the pretreatment level in the control group at 28 days post-induction, but remained similar to the pretreatment level in the KUS12 group. Additionally, the retinal thickness was significantly higher in the KUS121 group than in the control group at 14 and 28 days post-AION induction (day 28: RNFL + GCL thickness, 67.2 ± 4.7 µm vs. 46.1 ± 3.4 µm, $P = 0.003$; Fig. 2b–f, Supplementary Fig. S4). Hematoxylin and eosin staining at 28 days post-induction showed that KUS121 inhibited AION-induced thinning of inner retinal layers and prevented RGC loss (Fig. 2g–i). Moreover, retinal flat mounts showed that KUS121 treatment maintained the number of RGCs compared to the control (90.3 ± 14.4 cells vs. 62.5 ± 17.3 cells, $P = 0.062$; Fig. 2j–m).

Histological examination of the optic nerve in KUS121-treated AION rats

Considering that KUS121 treatment before AION induction (Fig. 1a) had a superior protective effect than that immediately after induction (Fig. 2a), KUS121 treatment before AION induction was adopted in subsequent experiments (Fig. 1a).

In addition to its effect on the inner retinal layers, we examined the neuroprotective effect of KUS121 on the optic nerve. Hematoxylin and eosin staining showed a disorganized medullary array in rats in the vehicle

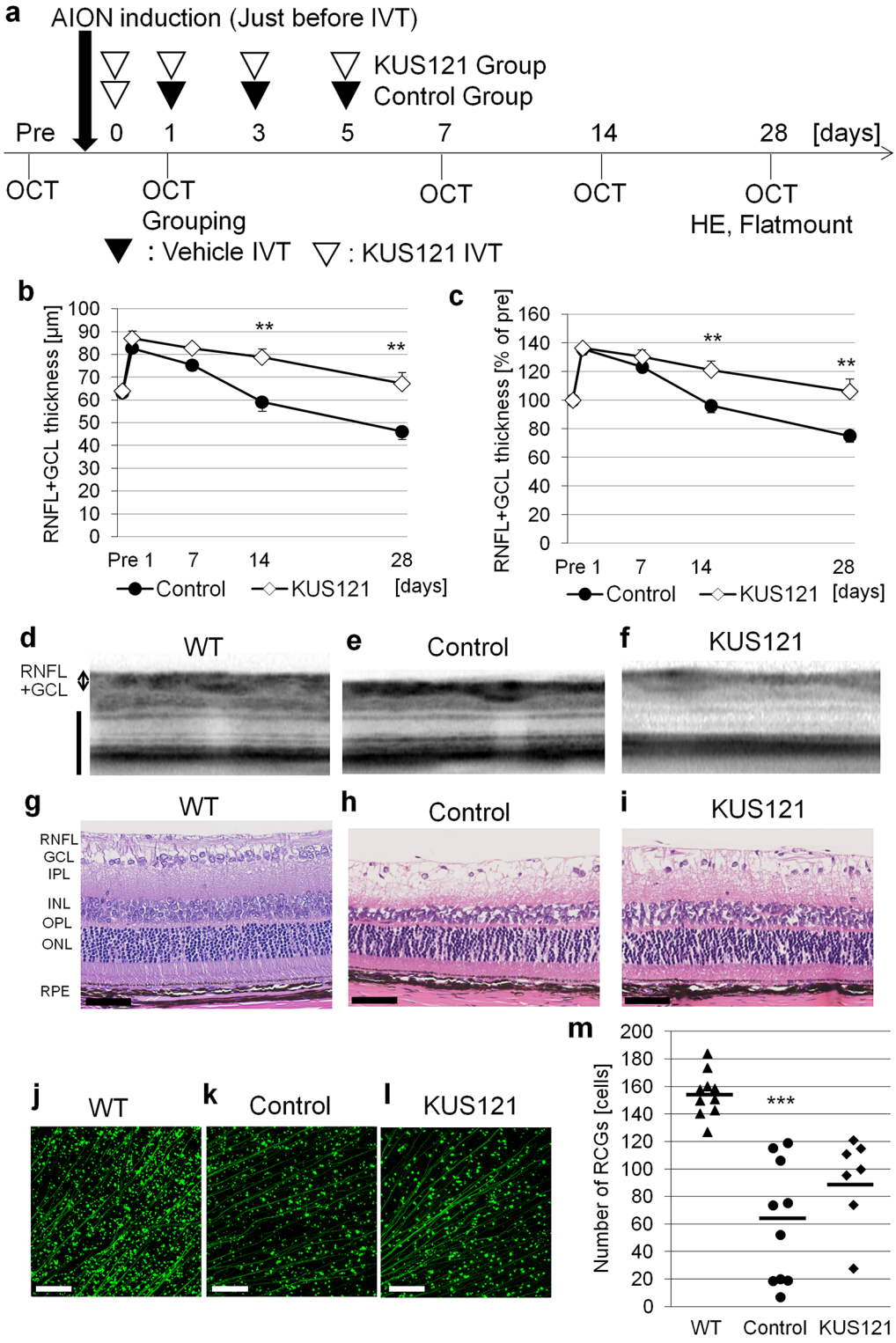

group compared with that in wild-type rats, and it was alleviated by KUS121 treatment (Fig. 3a, Supplementary Fig. S5a). Immunostaining with the anti-macrophage/monocyte antibody ED1 revealed significant infiltration of ED1-positive cells, including macrophages and potentially activated microglia, in the optic nerves of rats in the control group. In contrast, KUS121 treatment suppressed AION-induced infiltration of ED1-positive cells (Fig. 3b, g, Supplementary Fig. S5b). Similarly, the staining intensity of glial fibrillary acidic protein (GFAP), a marker of astrocytes, was higher in the optic nerve interstitium of rats in the control group than in that of rats in the KUS121 group; however, KUS121 treatment decreased GFAP staining intensity (Fig. 3c, h, Supplementary Fig. S5c). Additionally, microglia population was higher in the optic nerves of vehicle-treated rats with AION than in those of wild-type rats, as evidenced by an increase in the staining intensity of the microglia marker ionized calcium-binding adapter molecule 1 (Iba1). However, KUS121 treatment reduced microglia population in the optic nerves of rats with AION (Fig. 3d, i, Supplementary Fig. S5d). Neurofilament staining, an indicator

◀**Fig. 2**. Effects of post-induction intravitreal injections of KUS121 in a rat model of anterior ischemic optic neuropathy (rAION). **a** Schematic of experimental schedule. IVT: intravitreal injection. **b**, **c** Thickness of retinal layers, including the RNFL and GCL, (**b**) and the percent change compared to pre-treatment value (**c**) in AION rats injected with vehicle (control, $n = 8$, circles) or KUS121 ($n = 8$, squares). Error bars indicate SE. $^{**}P < 0.01$ vs. control (Student's t-test). **d–f** Representative OCT images of wild-type (WT, d) and AION rats injected with vehicle (control, **e**) or KUS121 (**f**). The double arrows indicate the layers, including the RNFL and GCL. Bar = 200 µm. **g–i** Representative HE-stained retinal sections of WT (**g**) and AION rats injected with vehicle (control, h) or KUS121 (i) at 28 days post-AION induction. Bar = 50 µm. **j–l** Representative images of flat-mounted retinas of WT (j) and AION rats injected with vehicle (control, k) or KUS121 (**l**) at 28 days post-AION induction. Bar = 100 µm. **m** Number of GFP-positive RGCs in flat-mounted retinas of WT ($n = 10$) and AION rats injected with vehicle (control, $n = 10$) or KUS121 ($n = 7$) at 28 days post-AION induction. GFP-positive RGCs were manually counted within four 500-µm squares located 2000 µm from the optic nerve head center (supplementary Fig. S1f). Bars indicate average. $^{***}P < 0.001$ vs. WT (Tukey's HSD test).

of neuron and ganglion cell population, showed minimal expression in the optic nerves of vehicle-treated rats with AION. In contrast, KUS121 treatment increased neurofilament staining intensity (Fig. 3e, Supplementary Fig. S5e). Additionally, Klüver–Barrera (KB) staining revealed disorganized myelin in the optic nerves of vehicle-treated rats with AION; however, KUS121 treatment ameliorated AION-induced changes in myelin sheaths (Fig. 3f, Supplementary Fig. S5f). Collectively, these results indicate that KUS121 treatment suppresses macrophage and microglia infiltration into the optic nerve and preserves neuronal integrity and myelin sheaths in rats with AION.

Electron microscopy confirmed myelin loss, swelling, thickening, and dilation, and uneven size and thickness of myelin sheaths in vehicle-treated rats with AION (Fig. 4a–d, g, h). In contrast, KUS121 treatment ameliorated AION-induced abnormalities in myelin sheaths (Fig. 4e–h).

Mechanisms underlying the neuroprotective effects of KUS121 in AION

In this study, we investigated the role of ER stress in AION pathology and the mechanisms underlying the neuroprotective effect of KUS121. Compared to untreated wild-type rats, vehicle-treated rats exhibited a trend toward increased level of C/EBP homologous protein (CHOP) at 1 day post-AION induction, but the difference was not significant between the groups ($P = 0.064$, Fig. 5a, b). However, KUS121 treatment significantly decreased CHOP protein level in the rats at 1 and 3 days post-AION induction ($P < 0.05$, control vs. KUS121). On day 5, although the difference was not significant, the mean CHOP protein level was lower in the KUS121 group than in the control group (CHOP, control: 1.21 ± 0.33, KUS121: 0.91 ± 0.17, $P = 0.28$, Fig. 5a, b). Similarly, in the immunohistochemical assay, the CHOP fluorescence intensity in the RNFL+GCL appeared lower in the KUS121 group than in the control group on day 5, but the difference was not significant (control: 43.9 ± 11.4, KUS121: 22.6 ± 8.2, $P = 0.20$, Fig. 5c–f).

Discussion

In this study, we investigated the neuroprotective effect of intravitreally administered KUS121 in rats with AION. Notably, KUS121 administration before and after AION induction significantly reduced the thinning of inner retinal layers and the loss of RGCs, demonstrating its neuroprotective effects. These benefits are likely mediated by the suppression of ER stress, a key factor in ischemia-induced neuronal death.

The pathogenesis of ischemic neuronal cell death involves apoptotic pathways triggered by ER stress[4,5]. Previous studies have shown that KUS121 alleviates ER stress and that it has anti-apoptotic effects, which slow disease progression in ocular conditions, such as retinitis pigmentosa and glaucoma[8–11], as well as in systemic diseases such as osteochondral[17,18]and ischemic renal diseases[19]. Additionally, KUS121 mitigates ischemic damage in flap ischemia models[20], further supporting its potential as a therapeutic agent for ischemic-related conditions. In this study, we confirmed that KUS121 reduced ER stress in RGCs, supporting its neuroprotective role. KUS121 has also shown neuroprotective effects, improving visual function in a retinal ischemia model[10]and in a clinical trial involving patients with central retinal artery occlusion[12]. However, the ERG analysis did not reveal any visual impairment in our rAION model, where the primary damage was to the inner retinal layers, preventing us from evaluating the effect of KUS121 on visual function.

Intravitreal administration of drugs is advantageous for retinal diseases as it ensures drug delivery directly to the retina, bypassing systemic circulation and achieving higher retinal concentrations, especially in ischemic conditions with impaired retinal blood supply. In the present study, KUS121 effectively preserved retinal morphology by protecting RGCs from ischemia-induced cell death in an rAION model. The histological analysis showed that KUS12 significantly reduced retinal thinning, a commonly observed change post-AION, supporting its neuroprotective role in RGC preservation. As stated by Guo et al.[21], the correlation between retinal swelling and RGC loss remains unclear. In addition to evaluating retinal thickness, we quantified RGCs using genetic labeling to further investigate the protective effects of KUS121 on RGCs.

Notably, KUS121 administration immediately after AION induction was effective in exerting neuroprotection. Although we acknowledge that the AION lesion takes several hours to fully develop, our findings show that treatment immediately after induction can mitigate subsequent damage. This finding provides insights into the therapeutic window during which neuroprotection is achievable. However, further research is necessary to examine the effect of treatment initiation one or more days after AION induction. To address variability in AION induction among animals, the rats were grouped based on total retinal thickening 1 day post-induction to minimize bias. KUS121 was administered immediately after AION induction to ensure consistency and avoid

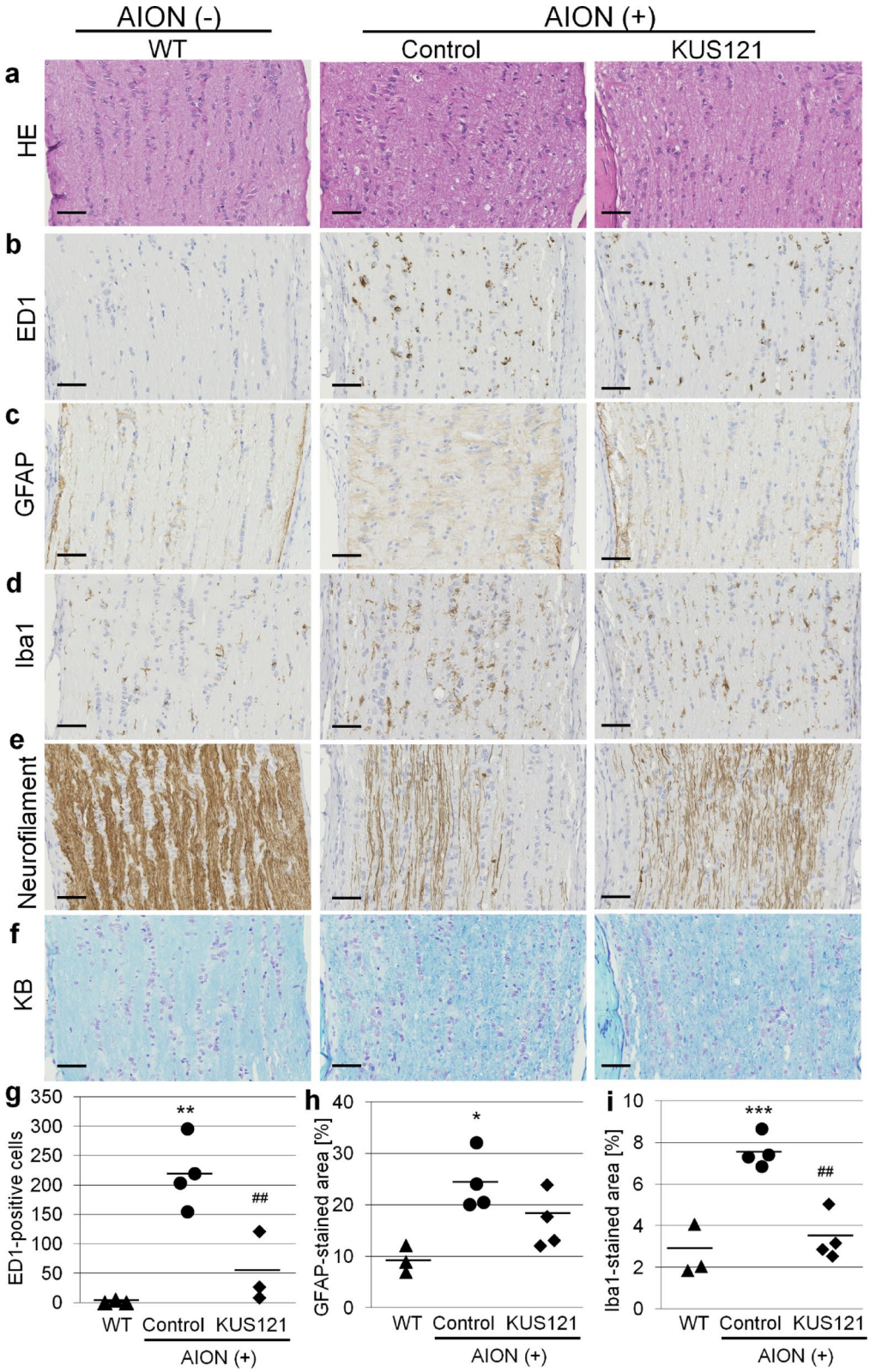

treatment delays, with group (vehicle vs. KUS121) assignment determined the following day. This experimental design may have contributed to the lack of significant differences in RGC counts between the groups, despite observable trends. Overall, these results suggest that KUS121 has a neuroprotective effect.

Our findings suggest that intravitreal administration of KUS121 not only preserves retinal morphology but also holds therapeutic potential for other retinal neurodegenerative diseases, particularly those involving impaired retinal blood supply. Conclusively, KUS121, a VCP modulator, exerted neuroprotective effects in a rat model of AION by suppressing ER stress and preserving retinal morphology. Our study offers a promising therapeutic approach for ischemic optic neuropathy and other neurodegenerative ocular diseases.

◀**Fig. 3**. Protective effect of KUS121 on the optic nerve of a rat model of anterior ischemic optic neuropathy (rAION). Histological examination of optic nerve sections in wild-type (WT), vehicle-treated AION (control), and KUS121-treated AION (KUS121) rats 28 days post-AION induction. Images of hematoxylin–eosin (HE)-stained sections (**a**); sections immunostained with anti-macrophage (ED1) (**b**), glial fibrillary acidic protein (GFAP) (**c**), ionized calcium-binding adapter molecule 1 (Iba1) (**d**), and neurofilament (**e**); and sections stained with Klüver–Barrera (KB) solution (**f**). Cells were counterstained with hematoxylin or cresyl violet. Bar = 50 µm. See Supplementary Fig. S5 for low-magnification images. **g-i** Number of ED1-positive cells (g, WT: 1.3 ± 0.8 cells, control: 217.8 ± 14.6 cells, KUS121: 51.7 ± 20.2 cells), and proportion of GFAP- (**h**, WT: 9.3 ± 0.9%, control: 24.1 ± 1.4%, KUS121: 16.7 ± 1.4%) and Iba1-stained areas (I, WT: 2.7 ± 0.4%, control: 7.6 ± 0.2%, KUS121: 3.4 ± 0.3%). WT: $n = 3$, control: $n = 4$, KUS121: $n = 3$ in g, $n = 4$ in h, i. Bars indicate average. $^{*}P < 0.05$, $^{**}P < 0.01$, $^{***}P < 0.001$, WT vs. control (Tukey's HSD test), $^{\#\#}P < 0.01$ control vs. KUS121 (Tukey's HSD test).

Methods

Compliance with guidelines

This study has been reported in accordance with the Animal Research: Reporting of In Vivo Experiments (ARRIVE) guidelines. All procedures adhered to the Association for Research in Vision and Ophthalmology statement for the Use of Animals in Ophthalmic and Vision Research. All protocols were approved by the Institutional Review Board of Kyoto University Graduate School of Medicine (MedKyo 15531,16501).

Experimental animals

We used *Thy1*-GFP transgenic rats[13], which express GFP in ganglion cells, including RGCs, under the control of neuron-specific elements of *Thy1*. These transgenic Sprague–Dawley rats were gifted by Dr. Christina K. Magill and Dr. Susan E. Mackinnon at Washington University[14].

The rats were housed under a 12:12-h light–dark cycle and provided with food and water ad libitum. *Thy1*-GFP rats with black eyes were generated by mating transgenic Sprague–Dawley rats with Brown Norway rats (Jackson Laboratory Japan Inc.). Rats obtained after 6–8 generations of backcrossing were used in this study. Male and female rats, approximately 8 weeks old and weighing 180–200 g, were used in the experiments. Before each experiment, the rats were anesthetized via intramuscular injection of ketamine (75 mg/kg) and xylazine (5 mg/kg). Pupil dilation was achieved with 0.5% tropicamide and phenylephrine eye drops. For the euthanasia procedure, deep anesthesia was induced via intramuscular injection of ketamine (75 mg/kg) and xylazine (5 mg/kg). This step was followed by the preparation of flat mounts, tissue collection for histological analysis, and retinal collection for western blotting. All other euthanasia procedures were performed using carbon dioxide.

Induction of AION

Rose Bengal (1.25 mM in phosphate-buffered saline, 5 mL/kg body weight) was injected into the tail vein of anesthetized rats. Immediately after the injection, laser photocoagulation was applied to the optic disc using a low-energy transpupillary laser (DC-3000; Nidek, Gamagori, Japan) with 500-µm diameter spots at 80-mW power for 12 seconds[15]. The power setting of 80 mW was determined based on preliminary experiments in which laser powers ranging from 50 to 120 mW were tested. Although power levels ≥ 90 mW resulted in severe retinal destruction, 80 mW induced sufficient retinal thinning for drug efficacy evaluation. Cover glasses were placed on the cornea as contact lenses during the procedure. To ensure consistency and improve reproducibility, all AION induction procedures were performed by the same individual.

Intravitreal injection of KUS121

KUS121 was dissolved in sterile water to obtain a 5 mg/mL solution. For intravitreal injections, 5 µL of KUS121 (25 µg/eye) or sterile water was injected intravitreally into the eyes of *Thy1*-GFP rats using a 33-gauge needle (Hamilton). In the pre-injection experiment, 12 rats from each group received KUS121 (25 µg/eye) or sterile water (control group). AION was successfully induced in the rats 30 min after injection. Additional intravitreal injections of the respective solutions were administered at 1, 3, and 5 days post-AION induction (Fig. 1a).

In the post-AION induction experiment, KUS121 was administered intravitreally immediately after AION induction. OCT imaging of the peripapillary retina was performed 1 day post-AION induction. To remove any biases, the rats were organized in the ascending order of total retinal thickness 1 day post-AION induction and alternately assigned to the control ($n = 11$) and KUS121 ($n = 10$) groups. KUS121 (25 µg/eye/day) or sterile water was intravitreally administered at 1, 3, and 5 days post-induction (Fig. 2a).

OCT image acquisition and retinal thickness measurement

Spectral-domain OCT examinations were performed on *Thy1*-GFP rats[10] before and at 1, 7, 14, and 28 days post-AION induction using Multiline OCT (Spectralis HRA + OCT, Heidelberg Engineering). Total retinal thickness, inner retinal thickness (comprising the RNFL, GCL, and IPL), and RNFL + GCL were measured using circular scan images along a circle 0.944 mm in diameter, centered on the optic nerve head (Supplementary Fig. S1a). The software for drawing boundary lines was a part of the built-in Spectralis HRA + OCT system provided by Heidelberg Engineering, to facilitate the manual assessment of B-scan images[10]. The mean thickness for each circular scan was calculated using this software.

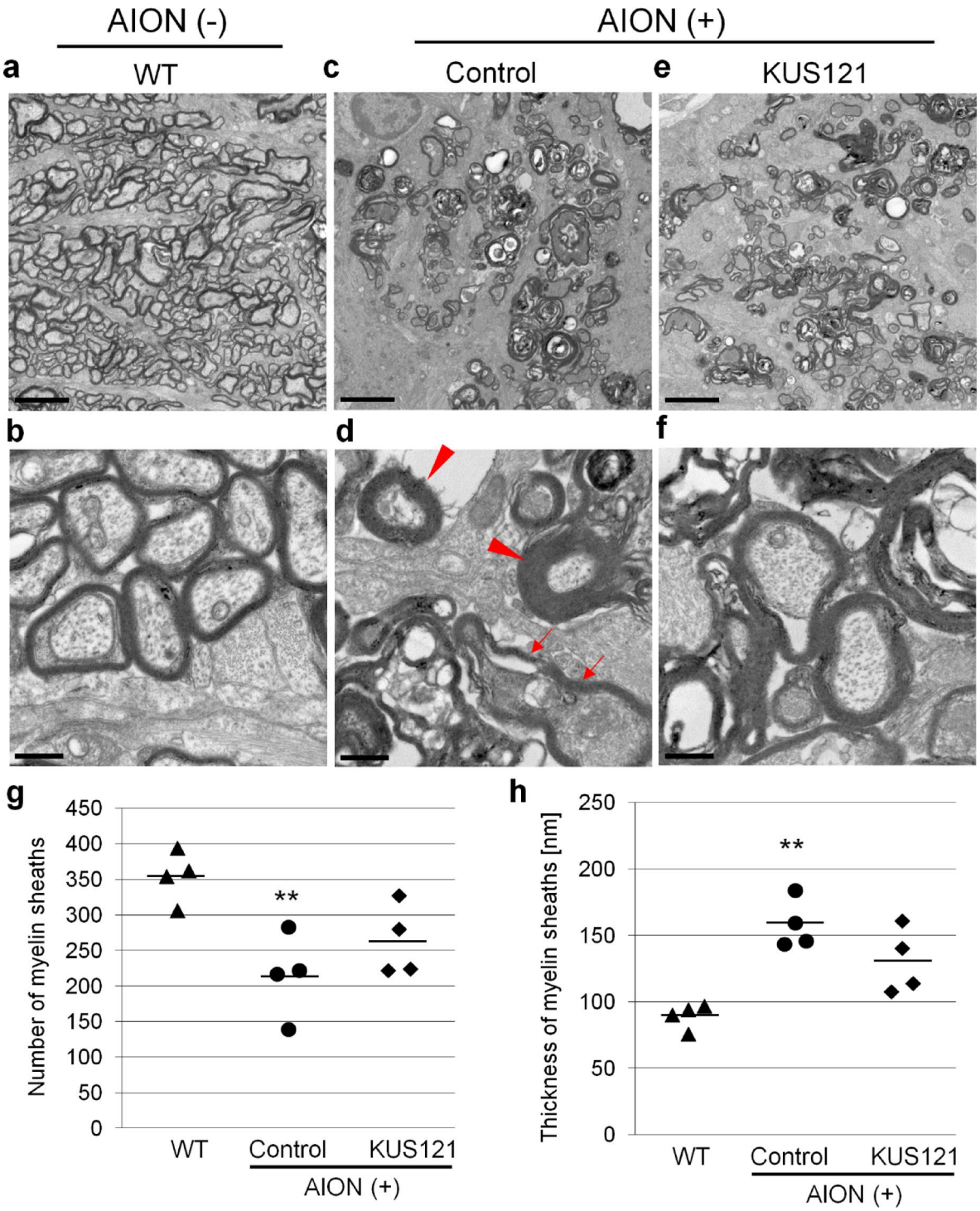

Fig. 4. KUS121 ameliorates myelin degeneration in the optic nerve of rats with anterior ischemic optic neuropathy (AION). Electron microscopy images of the optic nerve of wild-type (WT, **a**, **b**), vehicle-treated (control, **c**, **d**), and KUS121-treated rats (KUS121, **e**, **f**) 56 days post-AION induction. The arrowheads indicate myelin sheath thickening and arrows indicate myelin sheath expansion. Bar = 5000 nm in (a), (c), and (e); 500 nm in (b), (d), and (f). **(g)** Myelin sheaths were counted per image in an area of 746 μm^2. **h** Myelin sheath thickness was measured for 10 individual myelin sheaths per image in an area of 11 μm^2, and the average thickness was calculated. Thickness of myelin sheaths: WT: 89.2 ± 2.3 nm, control: 158.1 ± 4.6 nm, KUS121: 130.7 ± 6.2 nm.**$P < 0.01$ (Tukey's HSD test), $n = 4$. Bars indicate average.

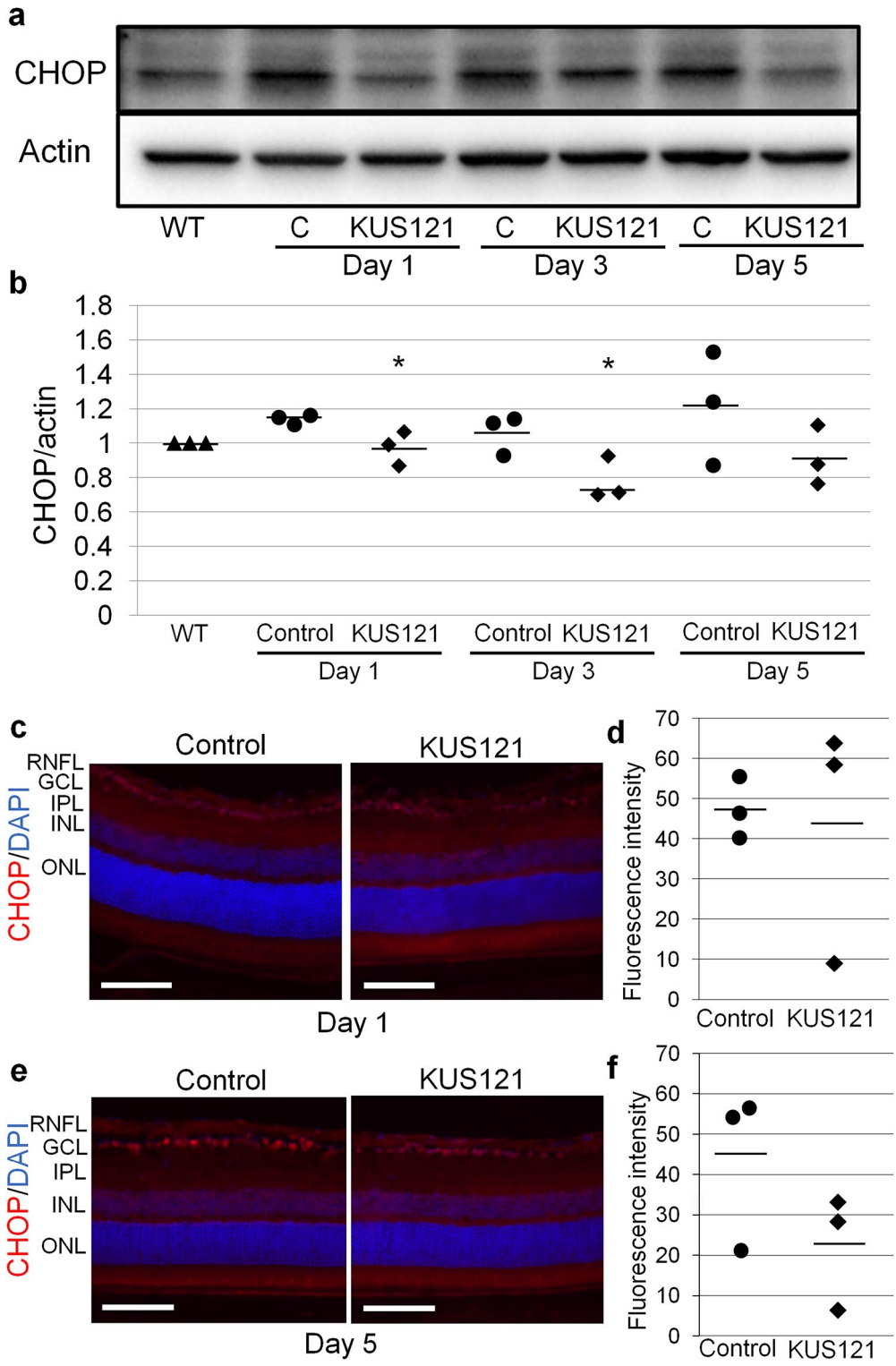

Fig. 5. KUS121 suppresses endoplasmic reticulum stress in rats with anterior ischemic optic neuropathy (AION). **a**, **b** Western blotting for C/EBP homologous protein (CHOP) and beta-actin expression in the retina before, and 1, 3 and 5 days post-AION induction (each group, $n = 3$). Complete scans of western blots are shown in Supplementary Fig. S6. Bars indicate average. *$P < 0.05$, vs. vehicle-treated AION rat (Tukey's multiple comparison test). **c**-**f** CHOP immunostaining (red) at 1 (c, d) and 5 days (**e**, **f**) post-AION induction. The nuclei were counterstained with 4',6-diamidino-2-phenylindole (DAPI, blue). **d**, **f** Comparison of average fluorescence intensity in the RNFL+GCL at 1 (d) and 5 days (f) post-AION induction. Student's *t*-test. Bars indicate average. (each group, $n = 3$). WT: normal rat, C: vehicle-treated AION rat, KUS121: KUS121-treated AION rat. Bar = 100 µm.

RGC counting in flat-mounted retinal images

GFP-positive retinal cells were assessed using whole-mounted retinal tissue samples. Twenty-eight days after AION induction, the eyeballs were enucleated, and the retinas were mounted and examined under a fluorescence microscope (BZ9000; KEYENCE). GFP-positive RGCs were manually counted in four 500-μm squares located 2000 μm from the center of the optic nerve head in the flat-mounted retinal images (Supplementary Fig. S1f). Counting was performed in a blinded manner, and the RGC counts from the four squares at 90-degree intervals around the optic nerve were averaged.

Histological analyses

Eyeballs with optic nerves were enucleated 28 days post-AION induction, fixed in Davidson's fixative for 24 h at room temperature, and embedded in paraffin for histological analysis. Serial 3-μm paraffin-embedded tissue sections were cut sagittally through the center of the optic nerve head and stained with hematoxylin-eosin. Additional sections were subjected to immunostaining following antigen retrieval in citric acid buffer (pH 6.0) in a microwave for 6 min. Klüver–Barrera staining was performed using the Luxol fast blue method.

For the histological analysis of CHOP, the eyeballs were enucleated 5 days post-AION induction, fixed in 4% paraformaldehyde at 4 °C for 24 h, embedded in paraffin, and sectioned into 6-μm sagittal slices through the center of the optic nerve head. The primary antibodies used were mouse anti-macrophages/monocytes (clone ED-1, 1:200; Millipore), mouse anti-GFAP (1:50; Dako), rabbit anti-Iba1 (1:1000; Wako), mouse anti-neurofilament (1:50; Dako), and rabbit anti-CHOP (1:200; Santa Cruz). The secondary antibodies used were Simple Stain rat MAX-PO(Multi) (NICHIREI BIOSCIENCES, Tokyo, Japan) and Alexa Fluor 594 goat anti-rabbit (1:1000; Thermo Fisher, Tokyo, Japan). The sections were stained using a DAB Kit (NICHIREI BIOSCIENCES) and observed with a Nanozoomer microscope (Nikon Solutions, Tokyo, Japan). CHOP-stained sections were counter-stained with 4',6-diamidino-2-phenylindole and examined using fluorescence microscopy (BZ9000; KEYENCE, Osaka, Japan).

ED1-positive cells per field (average field area: 120,000 μm^2) were counted within a region centered 1 mm from the optic nerve head. GFAP- and Iba1-stained areas were quantified as the percentage of the positive area per field within the same region. Additionally, CHOP staining intensity in the RNFL + GCL was measured within a range of approximately 713 μm in width.

Transmission electron microscopy

Briefly, optic nerves collected 56 days post-AION induction were fixed in 2.5% glutaraldehyde in phosphate-buffered saline, post-fixed in 2% osmium tetroxide with veronal acetate buffer, dehydrated in ethanol, and embedded in Epon 812 resin (TAAB Laboratories, Aldermaston, UK). Thereafter, the samples were cut into ultrathin sections, mounted on copper grids, and examined under an H-7770 transmission electron microscope (Hitachi, Tokyo, Japan). Myelin sheaths were counted per image with an area of 746 μm^2. Additionally, myelin sheath thickness was measured for 10 individual myelin sheaths per image with an area of 11 μm^2, and the average thickness was calculated.

Western blotting

After enucleation, the eyeballs were immersed in cold Hank's balanced salt solution. Small incisions were made in the cornea, and the choroid and retinal pigment epithelium were peeled away to isolate the neural retina. The lenses and iris were removed. Nine retinas from each time point (1, 3, and 5 days post-AION induction) were compared with those of untreated rats. The neural retina was lysed using radio-immunoprecipitation assay (RIPA) buffer containing protease and phosphatase inhibitors. Protein concentration was measured using a bicinchoninic acid assay, and 5 μg of protein was used for western blotting. The primary antibodies used were rabbit anti-CHOP (1:200; Santa Cruz) and anti-actin antibodies (1:5000; Sigma-Aldrich). The secondary antibodies used were horseradish peroxidase-conjugated anti-mouse IgG (1:5000) and horseradish peroxidase-conjugated anti-rabbit IgG (1:5000), with actin serving as the loading control.

Statistical analysis

Comparisons between rats treated with and those not treated with KUS121 were made using either the Aspin–Welch *t*-test or Student's *t*-test, depending on variance equality. Statistical comparisons among more than three experimental groups were performed using analysis of variance, followed by Tukey's multiple comparison test. Statistical analyses were conducted using EXSUS version 10.0.3 (SAS®9.4), and a significance level of $P < 0.05$ was considered.

Data availability

Data sharing is limited to research purposes, and we will consider requests for access. Requests for data access should be directed to Hanako Ikeda.

Received: 30 October 2024; Accepted: 18 April 2025
Published online: 27 April 2025

References

1. Hayreh, S. S. Ischemic optic neuropathies - where are we now? *Graefes Arch. Clin. Exp. Ophthalmol.* **251**, 1873–1884. https://doi.org/10.1007/s00417-013-2399-z (2013).
2. Hayreh, S. S. Ischemic optic neuropathy. *Prog Retin Eye Res.* **28**, 34–62. https://doi.org/10.1016/j.preteyeres.2008.11.002 (2009).
3. Hayreh, S. S. Controversies on neuroprotection therapy in non-arteritic anterior ischaemic optic neuropathy. *Br. J. Ophthalmol.* **104**, 153–156. https://doi.org/10.1136/bjophthalmol-2019-314656 (2020).

4. Tajiri, S. et al. Ischemia-induced neuronal cell death is mediated by the Endoplasmic reticulum stress pathway involving CHOP. *Cell. Death Differ.* **11**, 403–415. https://doi.org/10.1038/sj.cdd.4401365 (2004).
5. Li, H., Zhu, X., Fang, F., Jiang, D. & Tang, L. Down-regulation of GRP78 enhances apoptosis via CHOP pathway in retinal ischemia-reperfusion injury. *Neurosci. Lett.* **575**, 68–73. https://doi.org/10.1016/j.neulet.2014.05.042 (2014).
6. Hata, N., Oshitari, T., Yokoyama, A., Mitamura, Y. & Yamamoto, S. Increased expression of IRE1alpha and stress-related signal transduction proteins in ischemia-reperfusion injured retina. *Clin. Ophthalmol.* **2**, 743–752. https://doi.org/10.2147/opth.s3009 (2008).
7. Doh, S. H., Kim, J. H., Lee, K. M., Park, H. Y. & Park, C. K. Retinal ganglion cell death induced by Endoplasmic reticulum stress in a chronic glaucoma model. *Brain Res.* **1308**, 158–166. https://doi.org/10.1016/j.brainres.2009.10.025 (2010).
8. Ikeda, H. O. et al. Novel VCP modulators mitigate major pathologies of rd10, a mouse model of retinitis pigmentosa. *Sci. Rep.* **4**, 5970. https://doi.org/10.1038/srep05970 (2014).
9. Hasegawa, T. et al. Neuroprotective efficacies by KUS121, a VCP modulator, on animal models of retinal degeneration. *Sci. Rep.* **6**, 31184. https://doi.org/10.1038/srep31184 (2016).
10. Hata, M. et al. KUS121, a VCP modulator, attenuates ischemic retinal cell death via suppressing Endoplasmic reticulum stress. *Sci. Rep.* **7**, 44873. https://doi.org/10.1038/srep05970 (2017).
11. Muraoka, Y. et al. KUS121, an ATP regulator, mitigates chorioretinal pathologies in animal models of age-related macular degeneration. *Heliyon* **4**, e00624. https://doi.org/10.1016/j.heliyon.2018.e00624 (2018).
12. Ikeda, H. O. et al. Safety and effectiveness of a novel neuroprotectant, KUS121, in patients with non-arteritic central retinal artery occlusion: an open-label, non-randomized, first-in-humans, phase 1/2 trial. *PLoS One*. **15**, e0229068. https://doi.org/10.1371/journal.pone.0229068 (2020).
13. Magill, C. K., Moore, A. M., Borschel, G. H. & Mackinnon, S. E. A new model for facial nerve research: the novel Transgenic Thy1-GFP rat. *Arch. Facial Plast. Surg.* **12**, 315–320. https://doi.org/10.1001/archfacial.2010.71 (2010).
14. Bernstein, S. L., Guo, Y., Kelman, S. E., Flower, R. W. & Johnson, M. A. Functional and cellular responses in a novel rodent model of anterior ischemic optic neuropathy. *Invest. Ophthalmol. Vis. Sci.* **44**, 4153–4162. https://doi.org/10.1167/iovs.03-0274 (2003).
15. Chang, C. H., Huang, T. L., Huang, S. P. & Tsai, R. K. Neuroprotective effects of Recombinant human granulocyte colony-stimulating factor (G-CSF) in a rat model of anterior ischemic optic neuropathy (rAION). *Exp. Eye Res.* **118**, 109–116. https://doi.org/10.1016/j.exer.2013.11.012 (2014).
16. Danylkova, N. O., Alcala, S. R., Pomeranz, H. D. & McLoon, L. K. Neuroprotective effects of brimonidine treatment in a rodent model of ischemic optic neuropathy. *Exp. Eye Res.* **84**, 293–301. https://doi.org/10.1016/j.exer.2006.10.002 (2007).
17. Saito, M. et al. A VCP modulator, KUS121, as a promising therapeutic agent for post-traumatic osteoarthritis. *Sci. Rep.* **10**, 20787. https://doi.org/10.1038/s41598-020-77735-2 (2020).
18. Iwai, S. et al. KUS121 attenuates the progression of monosodium iodoacetate-induced osteoarthritis in rats. *Sci. Rep.* **11**, 15651. https://doi.org/10.1038/s41598-021-95173-6 (2021).
19. Hata, Y. et al. A novel VCP modulator KUS121 exerts renoprotective effects in ischemia-reperfusion injury with retaining ATP and restoring ERAD-processing capacity. *Am. J. Physiol. Ren. Physiol.* **322**, F577–F586. https://doi.org/10.1152/ajprenal.00392.2021 (2022).
20. Yoshimoto, K. et al. KUS121, a VCP modulator, protects against ischemic injury in random pattern flaps. *PLoS One*. **19**, e0299882. https://doi.org/10.1371/journal.pone.0299882 (2024).
21. Guo, Y., Mehrabian, Z., Milbrandt, J., DiAntonio, A. & Bernstein, S. L. Synergistic protection of retinal ganglion cells (RGCs) by SARM1 inactivation with CNTF in a rodent model of nonarteritic anterior ischemic optic neuropathy. *Cells* **13**, 202. https://doi.org/10.3390/cells13030202 (2024).

Acknowledgements

The authors thank Akiko Hirata for her contribution to the reliability assessment of RGC images. The authors thank Yumi Kuriki-Yamamoto, Toru Shibata, and Takaharu Mochizuki for technical assistance, and Takahisa Noto for technical and administrative support with the histological examinations. We also extend our gratitude to Professor Emeritus Nagahisa Yoshimura of Kyoto University and Takeshi Matsugi (Santen Pharmaceutical Co. Ltd.) for their administrative support. *Thy1*-GFP rats were a gift from Dr. Susan E. Mackinnon and Dr. Christina K. Magill of Washington University.

Author contributions

CK and HOI designed the research, conducted experiments, acquired, analyzed, and interpreted the data, and wrote the manuscript; SI conducted the experiments and acquired the data. MH and AT designed the study and interpreted the data.

Competing interests

Kyoto University has applied for patents related to this study (PCT/JP2011/067320&PCT/JP2011/073160), with Hanako Ohashi Ikeda and Masayuki Hata listed as inventors. Chinami Kikkawa is an employee of Santen Pharmaceutical Co., Ltd. A part of this study was conducted as a collaborative research project between Kyoto University and Santen Pharmaceutical Co., Ltd. All other authors declare that no competing interest.

Additional information

Supplementary Information The online version contains supplementary material available at https://doi.org/10.1038/s41598-025-99287-z.

Correspondence and requests for materials should be addressed to H.O.I.